ELSEVIER

Catalysis Today 39 (1997) 111–125

CATALYSIS TODAY

Highly active catalysts from inexpensive raw materials for coal gasification

Yasuo Ohtsuka[a,*], Kenji Asami[b]

[a] *Research Center for Organic Resources and Materials Chemistry, Institute for Chemical Reaction Science, Tohoku University, Sendai 980-77, Japan*

[b] *Department of Applied Chemistry, Faculty of Engineering, Osaka City University, Osaka 558, Japan*

Abstract

The present review article focuses on novel methods of converting inexpensive raw materials to active catalysts for low-temperature coal gasification, which can produce clean fuels and valuable feedstock with high thermal efficiency. Precipitation methods using NH_3, urea, and $Ca(OH)_2$ make it possible to prepare active, Cl-free iron catalysts on brown coals from an aqueous solution of $FeCl_3$ as the major component in acid wastes. The use of $Ca(OH)_2$ provides the most active iron, which achieves complete gasification within 60 min in a thermogravimetric run at 973 K. $Ca(OH)_2$ and $CaCO_3$ are other promising catalyst sources. $Ca(OH)_2$ promotes the steam gasification of many coals with different ranks at 973 K when kneaded with them in water. The calcium shows a larger catalytic effect for low-rank coals with higher contents of oxygen-functional groups as ion-exchangeable sites. $CaCO_3$, as a raw material of $Ca(OH)_2$, reacts with COOH groups to form ion-exchanged Ca and CO_2 when mixed with brown coals in water. Ion-exchange reactions proceed more readily with aragonite naturally present in seashells than with calcite from limestone. The exchanged calcium shows higher catalytic activity than the precipitated iron and provides at the largest 40–60-fold rate enhancement during steam gasification at 973 K. Catalysis of coal gasification by the iron and calcium is discussed in terms of catalyst dispersion, reactive sites, and sulfur poisoning. © 1997 Elsevier Science B.V.

1. Introduction

Catalytic gasification of coal has a great potential, since this process can produce environmentally acceptable fuels and chemical feedstock, such as H_2, CO, and CH_4, at low temperatures and with high thermal efficiency. A number of studies on catalytic gasification have been carried out from a fundamental and practical point of view, as shown in recent books and review papers [1–5]. It is generally accepted that potassium and other alkali metal compounds are the most active catalysts for steam gasification of coal, and K_2CO_3 was used in the Exxon catalytic coal gasification process to produce CH_4 directly from coal and steam [6,7]. However, there are some drawbacks with this catalyst; K_2CO_3 loses the activity by the reaction with inherent minerals such as quartz and kaolin and by vaporization as metallic potassium, and it is inactive at low temperatures of approx. 800 K where CH_4 formation is thermodynamically favorable.

We have reported that nickel catalyst finely dispersed on brown coal shows extremely high activity

*Corresponding author. Fax: (81-22) 217-5652; e-mail: ohtsukay@icrs.tohoku.ac.jp

PII S0920-5861(97)00093-X

for the steam gasification in such a low-temperature region [8,9], promotes efficient conversion of coal to very clean gas without tarry and sulfur materials [10], and achieves the direct production of CH_4-rich gas under the conditions of pressurized, fluidized-bed gasification [11]. Although 98% of the nickel used can be recovered from the gasification residue by the ammonia-leaching method using pressurized O_2 [10], the use of expensive nickel on a commercial scale is not easy, and the catalyst is readily deactivated by sulfur poisoning at 800–900 K [8].

Since several thousand tons of coal per day are gasified in a commercial process, abundance and inexpensiveness are indispensable requirements for catalyst raw materials. Therefore, our research interest has recently been directed toward the use of iron and calcium compounds as gasification catalysts. Iron is promising as an alternative to nickel. Iron chloride and sulfate are the most desirable catalyst sources, because these compounds are readily available as the major components in acid wastes from steel pickling and titanium oxide production plants [12]. When iron chloride and sulfate were added to coal by the conventional impregnation method, however, Cl- or S-containing gas inevitably evolves during gasification. This not only causes serious corrosion on various parts of materials but also increases the capacity needed for gas cleaning. The Cl- or S-free iron should thus be incorporated into coal particles.

With regard to the Ca-catalyzed gasification of coal, many studies have been carried out so far. Water-soluble compounds such as $Ca(CH_3COO)_2$, $Ca(NO_3)_2$, and $CaCl_2$ have been employed as catalyst precursors in most cases, because the addition method of impregnation and ion exchange can be used. However, $CaCO_3$, CaO, and $Ca(OH)_2$, which are naturally abundant as limestone and its derivatives, are suitable as raw materials. When these compounds are physically mixed with coal, their activities are quite low [13]. A novel method to convert these compounds to active catalysts should be developed.

From these standpoints, the present review article focuses mainly on the utilization of inexpensive raw materials, such as $FeCl_3$, $Ca(OH)_2$, and $CaCO_3$, as catalysts for steam gasification of coal. It can be expected that Fe and Ca cations interact with oxygen functional groups, such as carboxyl and phenolic groups, in coal structure, which essentially provides atomic-level dispersion and, consequently, leads to high activity for coal gasification. Therefore, low-rank coals with large amounts of oxygen functional groups are mainly used in the present study. Increasing energy demand in developing countries in Asia and Eastern Europe will force the use of low-rank coals, having huge reserves, in the future.

2. Experimental

2.1. Coal samples

Many coals with different ranks were used in the present study. Among them, Yallourn and Loy Yang brown coals from Victoria, Australia, were mainly used; they are denoted as YL and LY throughout this paper, respectively. All the samples were air-dried, ground, and sieved to coal particles with size fraction 75–150 or 150–250 μm. The proximate and ultimate analyses of YL and LY coals were almost the same; the ash contents were as low as < 1 wt% (dry), and the carbon and sulfur contents were 67–68 and 0.3 wt% (daf), respectively.

2.2. Catalyst material and addition

An aqueous solution of $FeCl_3$ was used mainly as a catalyst precursor among different iron compounds examined. The Fe ions in $FeCl_3$ solution were added to LY coal by the precipitation method using some bases. In order to examine the influence of precursor salts on the activity of iron catalyst, YL coal was impregnated with them by kneading it in their aqueous solutions with a mortar grinder [14].

In the preparation of calcium catalysts, $Ca(OH)_2$ and $CaCO_3$ were used unless otherwise described. $Ca(OH)_2$ was loaded onto various coals with different ranks by kneading them in the aqueous slurry, Ca loading being 5 wt% as the metal. The Ca ions in $CaCO_3$ with the two crystalline forms such as calcite and aragonite were exchanged with carboxyl groups in LY coal by simply mixing $CaCO_3$ powder and coal particles in deionized water at room temperature.

All the catalyst-loaded samples were dried at 380 K in a stream of N_2. Some of them were pelletized and then cut down to particles with size fraction 1–2 mm for convenience of gasification experiments.

2.3. Steam gasification

Isothermal gasification runs were carried out with a thermobalance equipped with infrared lamps, which made it possible to heat 20 mg of the sample at 300 K/min up to a predetermined temperature in a flow of steam (70–80 kPa) diluted with high-purity N_2 (> 99.9995%). The details of the procedure have been described elsewhere [14,15].

When the sample was heated rapidly as above, coal devolatilization first took place and was completed within a few minutes, and steam gasification of the devolatilized char proceeded subsequently [16]. The activity of every catalyst at the latter stage will be discussed throughout the present paper. Two indexes are used to describe the reactivity of char. One is char conversion, which is expressed as wt% on a dry ash free (daf), catalyst-free basis. Another is specific reaction rate, which is defined as the gasification rate per unit weight of remaining char.

2.4. Characterization

The amounts of Fe and Ca in the original and catalyst-loaded coals were determined by atomic absorption spectroscopy (AAS) after extraction of metals from the sample with hot HCl. The X-ray diffraction (XRD) measurements of catalyst-bearing coals and chars were made with Mn-filtered FeK_α or Ni-filtered CuK_α radiation for iron or calcium catalyst, respectively. The average crystallite size of catalyst species was determined by the Debye–Shörrer method. Fourier transform infrared (FTIR) spectra of the original and catalyst-loaded coals were measured by the diffuse reflectance method to examine interactions between coal and catalyst in the step of catalyst preparation. Mössbauer and X-ray photoelectron spectroscopy (XPS) measurements were performed for Fe-loaded samples at room temperature.

3. Results and discussion

3.1. Catalysis of steam gasification by iron

3.1.1. Precursor salts

Table 1 shows crystalline forms and dispersion of iron catalysts prepared onto YL coal from different precursor salts [14]. When the iron-loaded coal was devolatilized in an inert gas at 923 K, α-Fe with the small crystalline size of about 30 nm existed for iron ammonium oxalate and nitrate, and cementite (Fe_3C) also appeared. On the other hand, the reduction of iron sulfate and chloride to α-Fe was incomplete and the size of α-Fe was larger. Upon devolatilization in steam at 923 K, magnetite (Fe_3O_4) was the dominant species with all the catalysts. The crystalline sizes of magnetite were dependent strongly on the precursors and much smaller for iron oxalate and nitrate. The magnetite from the sulfate and chloride was too large to be determined by the Debye–Shörrer method. Thus, the dispersion of iron catalysts in the devolatilization step preceding the char gasification step depended on precursor salts.

Table 1
Characterization of iron catalysts derived from different precursor salts and their catalytic effects on char conversion during steam gasification [14]

Precursor salts [a]	Devolatilization in an inert gas [b]		Devolatilization in steam [b]		Char conversion after 2 h in steam at 923 K (wt%, daf)
	species [c]	size of α-Fe [d]	species [c]	size of Fe_3O_4 [d] (nm)	
None	—	—	—	—	23
$(NH_4)_3Fe(C_2O_4)_3$	α-Fe (s), Fe_3C (m)	32	Fe_3O_4 (s)	29	76
$Fe(NO_3)_3$	α-Fe (s), Fe_3C (m)	30	Fe_3O_4 (m), FeO (w)	10	82
$Fe_2(SO_4)_3$	FeO (s), FeS (m), α-Fe (w)	80	Fe_3O_4 (s), FeS (w)	> 100	25
$FeCl_3$	FeO (s), α-Fe (w)	> 100	Fe_3O_4 (s)	> 100	24

[a] Added to Yallourn brown coal at a loading of 10 wt% Fe.
[b] At 923 K.
[c] Identified by XRD: w – weak; m – medium; and s – strong.
[d] Determined by the Debye-Shörrer method.

Table 2
Conditions of preparation of iron catalysts from $FeCl_3$ solution and contents of iron, chlorine, and calcium in iron-loaded coals[a] [15,16]

Additives	Conditions of preparation		Content in coal [b]			Catalyst code
	temperature (K)	soaking time (h)	Fe (wt%)	Cl (wt%)	Ca (wt%)	
None [c]	370	8.0	0.95	0.66	—	Fe(hyd)
NH_3/NH_4Cl [d]	r.t. [e]	0.5	1.0	0.02	—	Fe(amm)
NH_3/NH_4Cl [d]	r.t. [e]	0.5	4.6	0.06	—	Fe(amm)
$(NH_2)_2CO$ [d]	370	4.0	3.4	0.04	—	Fe(ure)
$Ca(OH)_2$ [d]	r.t. [e]	0.5	1.0	—	0.16	Fe(cal)
$Ca(OH)_2$ [d]	r.t. [e]	0.5	4.7	0.04	0.51	Fe(cal)

[a] Loy Yang coal.
[b] Dry basis.
[c] Hydrolysis of $FeCl_3$.
[d] Precipitation method.
[e] Room temrerature.

Char conversion after steam gasification for 2 h at 923 K is also summarized in Table 1[14]. The catalysts from iron ammonium oxalate and nitrate promoted the gasification considerably. Char conversion increased from 23 wt% for the original coal to ca. 80 wt%. On the other hand, char conversions in the presence of iron sulfate and chloride were almost the same as that without iron, indicating that these compounds were almost inactive under the present conditions. When the iron-loaded coal was gasified with pure H_2, these four salts showed the same activity sequence as in steam [14].

The XRD and gasification results in Table 1 point out that the dispersion of iron catalyst upon devolatilization can determine the activity during subsequent char gasification, and the more highly dispersed iron is more active. Table 1 also reveals that iron chloride and sulfate, which are the major components in acid wastes, are not effective when simply impregnated with brown coal. It has been reported that these compounds can show catalytic activities under certain circumstances [17,18]. In these cases, however, Cl- or S-containing gas which evolved during gasification causes some serious problems, as already mentioned. A novel method for converting $FeCl_3$ to an active, Cl-free catalyst is described in the following section.

3.1.2. *Utilization of $FeCl_3$*

3.1.2.1. Catalyst preparation and analysis. Table 2 summarizes the conditions of catalyst preparation from an aqueous solution of $FeCl_3$ and the analyses of iron catalysts prepared [15,16]. The catalysts were precipitated onto LY coal by four different methods: by hydrolysis at 370 K and by use of NH_3 (buffer solution), urea ($(NH_2)_2CO$) and $Ca(OH)_2$ powder. These are denoted as Fe(hyd), Fe(amm), Fe(ure) and Fe(cal), respectively. The details of the procedure have been described elsewhere [15,16].

As is seen in Table 2, with the Fe(hyd) catalyst, only 1 wt% of Fe was loaded onto coal even when the concentration of $FeCl_3$ solution was increased, and some Cl was retained. On the other hand, most of the Fe cations in $FeCl_3$ solution could always be precipitated onto coal with Fe(amm), Fe(ure), and Fe(cal) catalysts, and the Cl contents in these samples were almost the same as that in the original coal, which means no Cl contamination. Slight amounts of Ca cations were retained in the Fe(cal) sample. The Ca retention originates from ion-exchange reactions between Ca ions in $Ca(OH)_2$ and carboxyl groups in LY coal [19,20].

3.1.2.2. Catalytic effect. Figs. 1 and 2 show the profiles for steam gasification of LY coal without and with iron catalysts at different temperatures [15,16]. The Fe(hyd) and Fe(amm) promoted the gasification even at small loadings of 1 wt% Fe, and char conversions with these catalysts at 973 K were larger than that without iron at 1023 K. The catalytic effect of the Fe(hyd) was comparable to that of the Fe(amm) at a higher loading of 4.6 wt% Fe. As is seen in Fig. 2, Fe(ure) was more active than Fe(hyd) and Fe(amm), and it exhibited almost

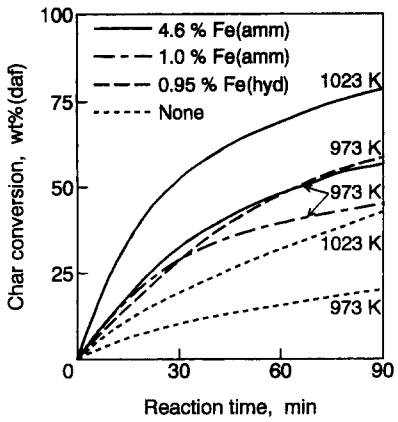

Fig. 1. Steam gasification profiles at 973 and 1023 K for Loy Yang coal without, and with iron catalysts [15,16].

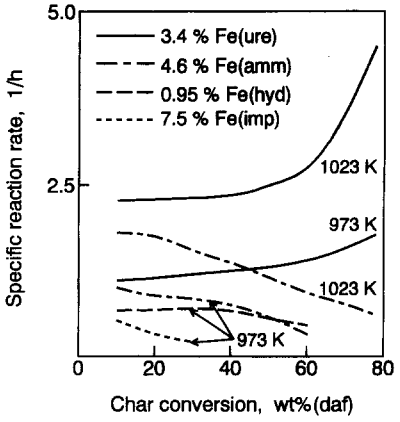

Fig. 3. Specific rate against char conversion for Loy Yang coal with several iron catalysts [15,16].

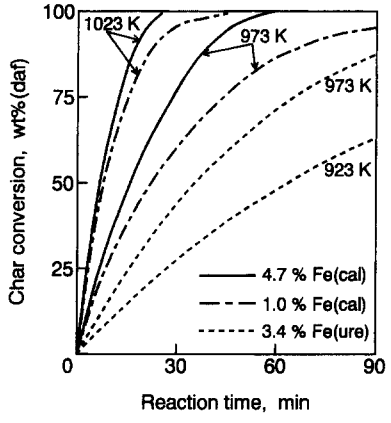

Fig. 2. Steam gasification profiles for Loy Yang coal with precipitated iron [16].

the same activity at 923 K as that of the Fe(amm) at 973 K. Thus, the reactivity of LY coal with the Fe(ure) at 923 K was larger than that for the original coal at 1023 K.

Fig. 2 also points out that Fe(cal) has the highest catalytic activity among the four types of iron examined; char conversion at 973 K reaches 95 wt% after 1.5 h at 1.0 wt% Fe and 100 wt% after 1 h at 4.6 wt% Fe. When the temperature was raised to 1023 K, only 40 wt% of char was gasified after 1.5 h in the absence of the catalyst, whereas the Fe(cal) achieved complete gasification within 45 and 25 min at loadings of 1.0 and 4.6 wt%, respectively. These observations lead to the following activity sequence:

$$\text{Fe(hyd)} \approx \text{Fe(amm)} < \text{Fe(ure)} < \text{Fe(cal)}$$

The specific reaction rate against char conversion is provided in Figs. 3 and 4. The rate at 973 K was lowest for the Fe(imp), prepared by the conventional impregnation method, despite the highest loading of 7.5 wt%, and it decreased rapidly with increasing char conversion. Such a rate drop has been reported by many workers [18,21,22] and is considered as the main drawback in the catalysis of coal gasification by iron. The rates with Fe(hyd) and Fe(amm) catalysts showed only a gradual decrease at 973 K after char conversion of ≈50 wt%. When the Fe(ure) catalyst

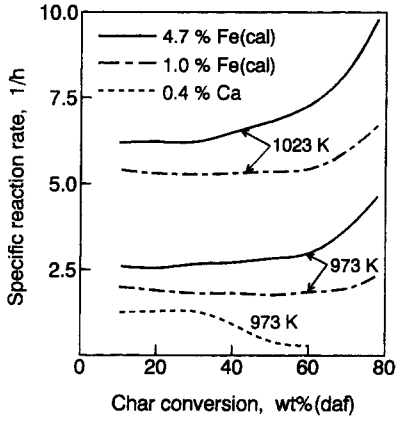

Fig. 4. Specific rate against char conversion at 973 and 1023 K for Loy Yang coal with iron and calcium [16].

was used, on the contrary, the rates increased as the gasification proceeded, and there was an exponential increase in the rate at 1023 K in the conversion range beyond 60 wt%.

The comparison of Figs. 3 and 4 indicates that the Fe(cal) provides the highest rate, regardless of temperature, and has almost the same rate profile as that with the Fe(ure). In other words, the rate for the Fe(cal) increased with increasing conversion irrespective of iron loading and reaction temperature. The rate at a higher loading or a higher temperature showed an exponential increase at the latter stage of gasification, as observed with the Fe(ure) catalyst.

As already mentioned, a small amount of the Ca (0.5 wt%) from $Ca(OH)_2$ as a precipitating agent was retained in the Fe(cal) sample (Table 2). Thus, almost the same amount of Ca was added to LY coal by ion exchange using a saturated solution of $Ca(OH)_2$. As is seen in Fig. 4, the exchanged Ca also promoted the gasification, but the catalytic effect was lower than that of the Fe(cal), and the rate with the Ca decreased rapidly beyond char conversion of 40 wt%, in contrast with a rate increase with the Fe(cal). Therefore, these observations show a minor contribution of residual Ca to the rate enhancement by the Fe(cal) catalyst.

Table 3 summarizes gasification rates and kinetic parameters [16]. Initial rates (R) at 1023 K with Fe(amm), Fe(ure), and Fe(cal) catalysts were 5, 6 and 18 times that for the original coal, respectively, and the rate enhancement indexes defined as $(R_{Fe} - R_{none})/R_{none}$, for these catalysts, were 4, 8 and 17, respectively. The degree of rate enhancement by the Fe(ure) and Fe(cal) increased with increasing char conversion in particular at the higher level, because the rates with these catalysts increased as the reaction proceeded (Figs. 3 and 4). As is seen in Table 3, the presence of Fe(amm), Fe(ure), and Fe(cal) catalysts lowered the apparent activation energy, determined from the Arrhenius plots using the initial rate, independently of catalyst type, and the degree of the lowering was larger for the latter two types of iron which showed larger catalytic activities [16].

One of several advantages of catalytic gasification is a lowering in reaction temperature. The degree of the lowering by iron addition can be evaluated from the difference in the temperature required for obtaining the same reaction rate with and without the catalyst, and it is summarized as ΔT in Table 3. The value of ΔT increased in the order of Fe(amm) < Fe(ure) < Fe(cal) [16], which agrees with the above-mentioned activity sequence. The use of the most effective Fe(cal) lowered the temperature by 140 K.

3.1.2.3. Catalyst state. When XRD measurements of Fe(amm), Fe(ure), and Fe(cal) catalysts precipitated onto LY coal were carried out, no XRD lines attributable to iron species were detectable [16], which strongly suggests that these catalysts are too fine to be determined by XRD.

Fe(amm), Fe(ure), and Fe(cal) were thus characterized by XPS and Mössbauer measurements. The results are summarized in Table 4. The binding energies of Fe $2p(3/2)$ observed were almost the same with all the catalysts and in good agreement with those for both a bulk compound of α-FeOOH and fine particles of FeOOH. On the other hand, the Mössbauer spectra of the Fe(amm) and Fe(cal) catalysts, showing a doublet in both cases, were quite different from those

Table 3
Gasification rates, kinetic parameters, and lowering in gasification temperature by iron addition

Catalyst	Fe (wt%)	R^a (1/h)	$(R_{Fe} - R_{none})/R_{none}$	Kinetic parameters [b]		ΔT^c (K)
				E_a (kJ/mol)	A (1/h)	
None	—	0.36	—	190	3.2×10^9	—
Fe(amm)	4.6	1.8	4.0	160	1.6×10^8	80
Fe(ure)	3.4	2.3	8.4	110	6.6×10^5	110
Fe(cal)	4.7	6.4	17	140	1.2×10^8	140

[a] Initial rate at 1023 K in the conversion range of ≤ 20%.
[b] E_a – apparent activation energy; A – frequency factor.
[c] Lowering in gasification temperature.

Table 4
Binding energies of Fe 2*p*(3/2) XPS spectra and Mössbauer parameters for iron catalysts precipitated on Loy Yang coal from $FeCl_3$ solution

Catalyst and references	Fe (wt%)	Fe 2p(3/2) [a] (eV)	Mössbauer parameters [b]		
			IS (mm/s)	QS (mm/s)	*H* (kOe)
Fe(amm)	4.6	711.0	0.39	0.97	0
Fe(ure)	3.4	711.2	—	—	—
Fe(cal)	4.7	711.3	0.39	0.79	0
α-FeOOH [c]	—	711.0	0.57	0.40	360
Fine FeOOH	—	711.2 [d]	0.41 [e]	0.89–0.91 [e]	0 [e]

[a] Corrected at C 1*s* peak of 284.6 eV.
[b] IS – isomer shift relative to α-Fe at room temperature; QS – quadrupole splitting; and *H* – hyperfine field.
[c] Commercial bulk compound (99.999% pure).
[d] FeOOH particles with the size of 3 nm supported on carbon.
[e] Fine particles of FeOOH dispersed on brown coal [25].

of bulk compounds of hydrated Fe_2O_3 and α-FeOOH [23,24]. As shown in Table 4, the values of Mössbauer parameters such as IS and QS with the Fe(amm) and Fe(cal) were nearly equal to those reported for fine particles of FeOOH dispersed on an Australian brown coal [25]. This agreement shows that these catalysts are present in the forms of finely dispersed FeOOH. It has been reported that fine particles of FeOOH are also formed by hydrolysis of $FeCl_3$ solution at elevated temperatures [26] and by homogeneous precipitation from aqueous solutions of iron chloride and sulfate using urea [27].

Unfortunately, the present precipitation method using $Ca(OH)_2$ and urea could not be successfully applied to sub-bituminous and bituminous coals with low oxygen contents [28]. This observation suggests that Fe ions interact strongly with free carboxyl groups, which are not associated with metal cations, during precipitation on brown coal. The FTIR spectra of the Fe(amm) catalyst showed the occurrence of ion-exchange reactions between some of the Fe ions and protons in carboxyl groups [15].

When LY coal samples with the Fe(amm), Fe(ure), and Fe(cal) catalysts at loadings of 3.4–4.7 wt% Fe were devolatilized in steam at 973 K, the XRD signals of magnetite (Fe_3O_4) alone appeared irrespective of catalyst type [16], as predicted from the phase diagram for Fe–H_2O–H_2 system [29]. The XRD intensities were low in all cases despite the relatively large contents of 7–9 wt% Fe in devolatilized chars. This indicates the low crystallinity of magnetite, that is, the high dispersion of every catalyst in the devolatilization step.

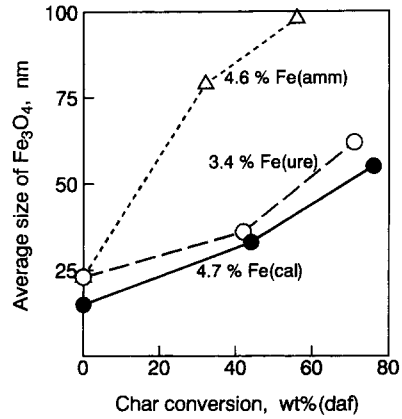

Fig. 5. Change in the average size of Fe_3O_4 with char conversion during gasification at 973 K (Reprinted with permission from [16]: Copyright (1993) American Chemical Society).

The chemical form of magnetite was retained throughout the subsequent char gasification and this was the only species detected by XRD. The change in the average crystalline size of magnetite with char conversion at 973 K is illustrated in Fig. 5 [16], where conversion of zero means devolatilization. The sizes for the three catalysts upon devolatilization were as small as 15–23 nm. As the reaction proceeded, the size increased in all cases because magnetite particles agglomerated due to the loss of char by gasification. However, the agglomeration rate depended strongly on the catalyst type and increased in the sequence of Fe(cal) < Fe(ure) ≪ Fe(amm). In other words, the degree of catalyst dispersion in the char gasification process was high in the

following order:

$$Fe(amm) \ll Fe(ure) < Fe(cal)$$

The rapid agglomeration of the Fe(amm) catalyst resulted in the decreased specific rate with char conversion (Fig. 3). On the other hand, the Fe(ure) and Fe(cal) catalysts were kept in the highly dispersed forms up to the latter stage of gasification, which can lead to the enrichment of catalyst species in the remaining char. As a result, the specific rates with these catalysts increased as the reaction proceeded (Figs. 3 and 4). The order of catalyst dispersion among the three types of iron also corresponded well to the above-mentioned activity sequence.

These findings show that the dispersion of magnetite particles during gasification is convenient for elucidating the catalytic behavior of precipitated iron. However, it does not necessarily mean that magnetite is the actual catalytically active species, since magnetite is the bulk form identified by XRD. The reducing gas such H_2 and CO evolved during steam gasification [15], and iron particles reacted readily with carbon in the char matrix to form iron carbides (Table 1). Thus, the surface of magnetite would actually be in a higher reduced state. It is likely that the iron-catalyzed gasification proceeds through the oxygen-transfer mechanism involving the redox-cycle of iron oxides [4,12,30,31].

3.2. *Catalysis of steam gasification by calcium*

3.2.1. *Precursor salts*

The influence of the kind of calcium compounds on the reactivity of YL coal in steam at 923 K is illustrated in Fig. 6 [32], where these are added at a loading of 5 wt% Ca by kneading with coal particles in deionized water. $Ca(CH_3COO)_2$, $Ca(NO_3)_2$, $Ca(OH)_2$, and $CaCO_3$ showed almost the same catalytic effect, and achieved complete gasification within 60–70 min. The catalyst effectiveness of these compounds was much higher than that of $Fe(NO_3)_3$ and $(NH_4)_3Fe(C_2O_4)_3$ (Table 1). $CaCl_2$ and CaS also promoted the gasification remarkably, though their activities were slightly lower. Their use is not feasible due to evolution of Cl- or S-containing pollutants. $CaSO_4$ was much less effective.

When YL coal with the most effective acetate, nitrate, and hydroxide was devolatilized in an inert

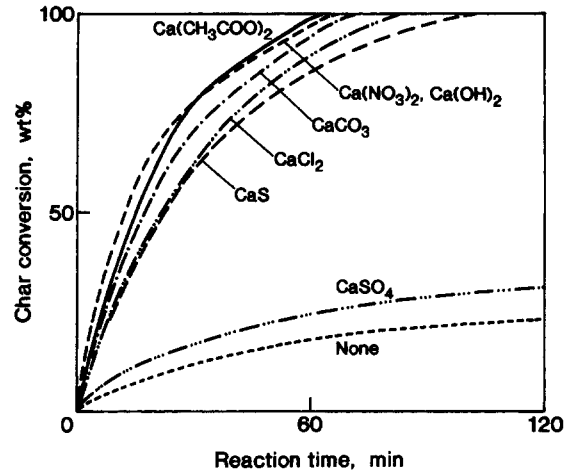

Fig. 6. Steam gasification of Yallourn coal with different calcium compounds at 923 K (Reprinted from Ref. [32] with kind permission from Elsevier Science, Amsterdam, The Netherlands).

Table 5
In situ XRD results for Ca-loaded coals during devolatilization in an inert atmosphere

Sample	Precursors [a]	Ca species upon devolatilization [b]	
		923 K	1023 K
Raw coal	$Ca(CH_3COO)_2$	n.d. [c]	CaO (18)
923 K-char [d]	$Ca(CH_3COO)_2$	CaO (> 100)	—
Raw coal	$Ca(NO_3)_2$	n.d. [c]	CaO (12)
Raw coal	$Ca(OH)_2$	n.d. [c]	CaO (11)
Raw coal	$CaSO_4$	$CaSO_4$	—

[a] Loading of 5 wt% Ca.
[b] Average crystallite size of CaO denoted in parentheses.
[c] Not detectable by XRD.
[d] Char devolatilized at 923 K before catalyst addition.

atmosphere, as shown in Table 5, the in situ XRD measurements revealed that no Ca species could be detected at 923 K, but very small and broad XRD peaks of CaO appeared at 1023 K, the average size of CaO being as small as 10–20 nm [20]. On the other hand, the impregnation of $Ca(CH_3COO)_2$ on the devolatilized char instead of the raw coal resulted in the formation of larger particles of CaO even at 923 K (Table 5), and the catalytic activity was quite low [20]. The poor dispersion is caused by the drastic decrease in the content of COOH groups as ion-exchangeable sites by devolatilization, from 1.9 to < 0.01 meq/g. In other words, the presence of COOH groups in coal is one of the key factors for controlling

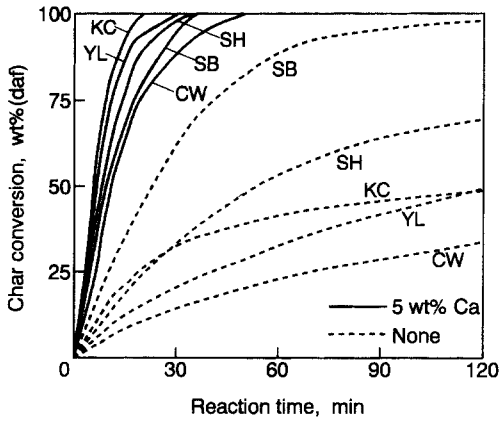

Fig. 7. Steam gasification profiles at 973 K for low-rank coals without and with $Ca(OH)_2$ [33]. Key as in Table 6.

catalyst dispersion and, consequently, catalytic activity.

It is evident in Fig. 6 that inexpensive $Ca(OH)_2$ and $CaCO_3$ are promising as catalyst raw materials. The details in the catalysis of coal gasification by these compounds are discussed below.

3.2.2. *Utilization of $Ca(OH)_2$*

3.2.2.1. Catalytic effect. Typical profiles for steam gasification at 973 K of different coals without and with $Ca(OH)_2$ are illustrated in Figs. 7 and 8 [33], where each coal is designated by a code name provided in Table 6. Figs. 7 and 8 respectively show the results for low- and high-rank coals, and their elemental analyses are simply summarized in Table 6.

As is seen in Fig. 7, the reactivities of low-rank coals without catalyst were relatively large and strongly dependent on the coal type. Larger reactivities were observed for SB and SH coals with higher contents of Ca naturally present in coal (Table 6). As is well known, Ca in low-rank coals exists mostly as the ion-exchangeable forms and promotes steam gasification [34,35]. The addition of $Ca(OH)_2$ led to complete gasification within 20–50 min in every case, but the catalytic effect differed widely among these coals.

When high-rank coals were gasified, as shown in Fig. 8, the reactivities in the absence of $Ca(OH)_2$ were much lower that those of low-rank coals and almost independent of the coal type. Relatively large amounts of inherent Ca were contained in IL and MK coals (Table 6), but Ca was present mostly as gypsum ($CaSO_4 2H_2O$) and, thus, almost inactive (Fig. 6). The use of $Ca(OH)_2$ promoted the gasification of all the coals examined, but the catalytic effect depended on the coal type, as observed in Fig. 7.

A rate enhancement index defined as $(R_{Ca} - R_{none})/R_{none}$ is convenient for comparing the rate enhancement by calcium addition quantitatively among low-rank coals [32]. Fig. 9 shows the relationship between

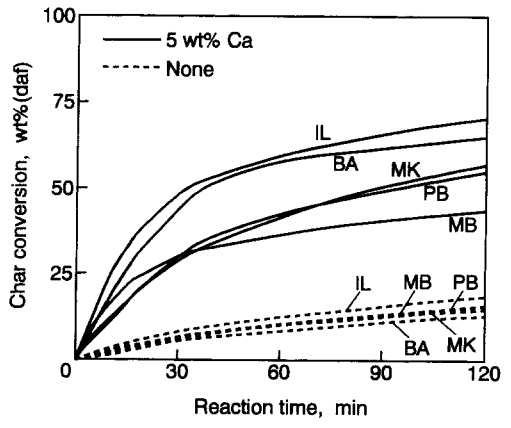

Fig. 8. Steam gasification profiles at 973 K for high-rank coals without and with $Ca(OH)_2$ [33]. Key as in Table 6.

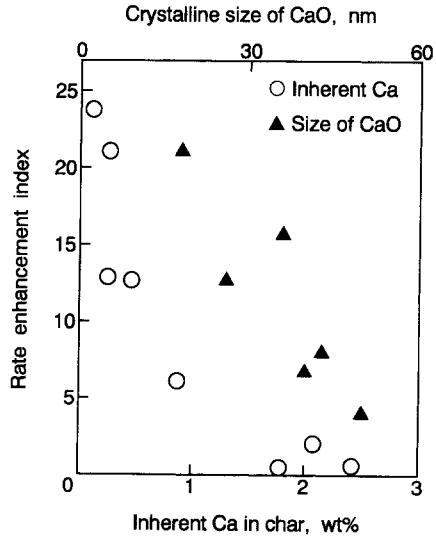

Fig. 9. Relationship between rate enhancement index and the content of inherent Ca in char or the average size of CaO [33].

Table 6
Analyses of some coals used, activation energies for steam gasification crystalline species of calcium catalysts and ratio of sulfur captured to calcium added upon pyrolysis [33]

Coal sample [a]	Content in coal [b] (wt%)			E_a [c] (kJ/mol)		XRD species of Ca catalysts [d]	S_{cap}/Ca_{add} [e]
	C	S	Ca	None	5 wt% Ca		
Yallourn (YL)	67.1	0.3	0.06	160	150	n.d. [f]	—
Shori (SH)	67.8	1.0	0.54	155	145	n.d. [f]	—
South Beulah (SB)	71.6	2.9	1.3	165	135	CaS (w)	0.15
Colowyo (CW)	74.0	0.4	0.17	185	135	CaO (w)	—
King Cannel (KC)	74.2	1.9	0.13	170	160	CaS (w)	0.09
Illinois No.6 (IL)	77.0	3.6	0.31	130	130	CaO (m), CaS (m)	0.09
Miller Blend (MB)	81.1	1.3	0.08	—	—	CaO (m)	—
Blair Athol (BA)	81.9	0.4	0.06	—	—	CaO (m)	—
Pittsburgh (PB)	83.4	2.4	0.10	—	—	CaO (m), CaS (s)	0.22
Miike (MK)	83.6	3.7	0.69	135	135	CaO (m), CaS (m)	0.06

[a] Code name designated in parentheses.
[b] C or S content on a dry, ash-free basis, and inherent Ca on a dry basis.
[c] Apparent activation energy.
[d] After devolatilization of Ca-loaded coals at 973 K in an inert atmosphere; XRD intensities designated as: w – weak; m – medium; and s – strong.
[e] Atomic ratio of S captured to Ca added during pyrolysis at 973 K.
[f] Not detectable by XRD.

the index at 973 K and the content of inherent Ca in char after devolatilization [33]. The index decreased rapidly with increasing the content, which indicates that the externally added Ca can work more effectively in the gasification of low-rank coals with smaller contents of inherently present Ca.

Table 6 summarizes the apparent activation energies calculated for seven coals by the Arrhenius plots using initial reaction rates [33]. The addition of $Ca(OH)_2$ either showed no effect on the activation energy or lowered it slightly in most cases, as has been observed in several studies on the Ca-catalyzed gasification [32,36,37]. This observation suggests that the catalysis of coal gasification by calcium is due to the increased number of reactive sites, irrespective of precursor salts. It has been shown by temperature-programmed desorption and transient kinetics measurements [38–40] that the highly dispersed Ca can interact strongly with carbon and promote the dissociation of O-containing gas and subsequent oxygen spillover, which results in the increased amount of surface oxygen complexes as reactive sites.

3.2.2.2. Catalyst state. The Ca-bearing chars after devolatilization of several coals with $Ca(OH)_2$ at 973 K were characterized by XRD. The results are shown in Table 6 [33]. No diffraction lines due to Ca species were detectable with YL and SH chars. As the rank of parent coals increased, CaO appeared and the XRD intensities increased. The average crystalline size of CaO also showed the same trend. These results point out that the addition of $Ca(OH)_2$ to low-rank coals with large amounts of ion-exchangeable sites leads to the increased dispersion of CaO particles, which corresponds to the higher dispersion of CaO derived from $Ca(CH_3COO)_2$ loaded on the raw YL coal than on the devolatilized char (Table 5). As shown in Fig. 9, the enhancement index was larger for the coals with the smaller size of CaO. It is likely that the more finely dispersed calcium is responsible for larger catalyst effectiveness observed with low-rank coals.

When $Ca(OH)_2$ was loaded on high sulfur coals such as SB, KC, IL, PB, and MK coals, CaS appeared and the diffraction intensities increased with increasing coal rank (Table 6). The formation of CaS means that the added calcium can capture the sulfur evolved upon devolatilization. As is seen in Table 6, however, the atomic ratio of the sulfur captured to the calcium added was always < 0.25, which indicates that $> 75\%$ of the calcium added is free from sulfur poisoning. Thus, there is less severe catalyst deactivation by sulfur. This can be supported by thermodynamic considerations that the present gasification conditions, such as a high partial pressure of steam and a low temperature of 973 K, are unfavorable to the reaction of CaO and H_2S [41]. On the other hand, the formation of CaS even under the differential reaction conditions suggests that, if a sufficient amount of $Ca(OH)_2$ is added to high sulfur coals, the calcium can work as not only a gasification catalyst but also an in situ desulfurization agent during coal gasification [42].

3.2.3. *Utilization of $CaCO_3$*

3.2.3.1. Ion exchange reactions between $CaCO_3$ and COOH groups. $Ca(OH)_2$ is manufactured by calcination of limestone ($CaCO_3$) and subsequent hydration of CaO formed. Utilization of $CaCO_3$ in place of $Ca(OH)_2$ as a catalyst raw material can, therefore, lead to a simplified catalytic gasification process. As mentioned above, $CaCO_3$ showed almost the same rate enhancement as $Ca(OH)_2$ when kneaded with YL coal in water (Fig. 6). It is well understood that the Ca^{2+} ions in a saturated solution of $Ca(OH)_2$ can readily undergo ion-exchange reactions with COOH groups in coal due to its strong basicity, and that the exchanged Ca shows high activity for steam gasification. However, it appears mysterious why $CaCO_3$ can work as effectively as the exchanged Ca derived from $Ca(OH)_2$. The present section thus makes clear the interactions between $CaCO_3$ and low-rank coals in water.

The conditions of ion exchange, using $CaCO_3$ with the two crystalline forms of calcite and aragonite, are simply summarized in Table 7. A predetermined amount of $CaCO_3$ powder was added to a mixture of LY coal and deionized, CO_2-free water, and the resulting mixture was stirred for 60 min under a flow of high-purity N_2 at room temperature. The details of the procedure have been described elsewhere [43]. Upon use of calcite from limestone, the pH of the mixture increased gradually with increasing stirring time and became ca. 6 after 60 min. When aragonite naturally present in seashells and coral reef was added,

Table 7
Conditions of ion exchange using $CaCO_3$, change in pH during ion exchange, and amounts of CO_2 evolved and Ca loaded

Conditions of ion exchange [a]		Change in pH with time [b]			CO_2 evolved and Ca loaded (mmol/g-coal)		
type of $CaCO_3$	Ca added (nmol/g-coal)	initial	2-min-soak	final	CO_2	Ca	CO_2/Ca
Calcite	1.3	3.9	4.5	6.2	0.41	0.56	0.73
Aragonite	1.3	4.0	6.5	6.9	0.63	0.84	0.75

[a] 10 g of Loy Yang coal and 150 cm^3 of deionized, CO_2-free water.
[b] Change in pH during 60 min-stirring after $CaCO_3$ addition to a mixture of coal and water at room temperature.

on the other hand, the pH increased steeply from the initial 4 to 6.5 after 2 min soaking, showed a gradual increase and, finally, reached the value of ca. 7.

As is seen in Table 7, the analysis of the gas, evolved during stirring, revealed the formation of a large amount of CO_2 irrespective of the crystalline form of $CaCO_3$, though the amount was larger with aragonite than with calcite. The amount of the Ca actually loaded onto LY coal, determined by AAS, was also higher with aragonite (Table 7). However, the ratio of the CO_2 evolved to the Ca loaded was almost the same between the two, that is, 0.73 and 0.75 for calcite and aragonite, respectively. These observations point out that CO_2 originates from ion-exchange reactions between $CaCO_3$ and LY coal.

Fig. 10 shows the FTIR spectra of the raw and Ca-loaded coals [43]. A strong, carboxylic C=O stretching band was observed at 1700 cm^{-1} for the raw coal without Ca. When LY coal was ion-exchanged with the Ca ions in calcite in the above-mentioned manner, the intensity of the IR peak at 1700 cm^{-1} decreased dramatically, and instead the intensity of the absorption band at ≈1600 cm^{-1} increased, the latter being attributable to carboxylate anions as well as C=O bonds inherently present in coal. Aragonite provided essentially the same spectrum as calcite. When calcite was kneaded with LY coal in deionized water, 3.9 wt% Ca was actually loaded on coal and the FTIR spectrum showed almost the same feature as in the exchanged samples (Fig. 10).

The results shown in Table 7 and Fig. 10 indicate that ion-exchange reactions between the Ca ions in $CaCO_3$ and the protons in COOH groups take place according to the following equation [43]:

$$CaCO_3 + 2(-COOH) = -(COO)_2Ca + CO_2 + H_2O$$

This equation shows that the molar amounts of the CO_2 evolved and the Ca exchanged should be equal,

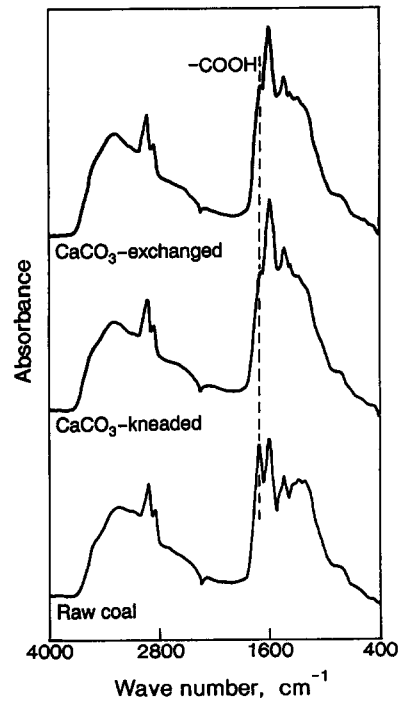

Fig. 10. FTIR spectra of Loy Yang coal with and without $CaCO_3$ (Reprinted with permission from [43]: Copyright (1996) American Chemical Society).

but the former was equivalent to ≈75% of the latter (Table 7), regardless of the type of $CaCO_3$. Higher amounts of the Ca observed, than that estimated from the CO_2 evolved, can be ascribed to incomplete removal of unreacted $CaCO_3$ from the Ca-exchanged coal in the separation process. Thus, the above equation probably proceeds stoichiometrically. Its detailed reaction scheme has been proposed elsewhere [43].

3.2.3.2. Catalyst state and activity. The XRD measurements showed the absence of any signals due to Ca species before and after devolatilization

Table 8
Effects of type of $CaCO_3$ and addition method on rate enhancement in steam gasification of Loy Yang brown coal at 973 K [43]

Addition of $CaCO_3$			R^a	$(R_{Ca} - R_{none})/R_{none}$
precursor	method	Ca (wt%)		
None	—	—	0.13	—
Calcite	physical mixing	3.9	0.30	1.3
Calcite	kneading	3.9	7.6	58
Calcite	ion exchange	2.2	5.4	40
Aragonite	ion exchange	3.3	8.0	61

[a] Initial rate.

of Ca-exchanged coals at 973 K. The X-ray absorption fine structures spectroscopy has revealed that the Ca ions exchanged with COOH groups are essentially atomically dispersed [44]. Upon devolatilization, the exchanged Ca is transformed into the well-dispersed species with fine crystallites of < 5 nm size [45], and these are thus not detectable by XRD. The highly dispersed species derived from calcite and aragonite can lead to the exceptionally high activity at a low temperature of 973 K, as will be mentioned in the following.

Table 8 summarizes gasification rates for Ca-loaded coals at 973 K [43]. The reactivity of LY coal with the physically-mixed carbonate was quite low. On the other hand, the kneaded carbonate exhibited high catalytic activity, as expected from Fig. 6. The carbonate also promoted the gasification of other brown coals and showed the larger effectiveness for the coals with higher contents of free COOH groups available as ion-exchangeable sites [43]. The exchanged Ca from calcite and aragonite worked as effectively as the kneaded calcite (Table 8). The initial rates for calcite and aragonite reached ca. 40 and 60 times that without the calcium, respectively. The larger reaction rate with aragonite, as opposed to calcite, may be ascribed to a higher Ca loading, since the gasification rate of carbon in the presence of ion-exchanged Ca increases linearly up to catalyst loading equivalent to the amount of COOH groups [46].

When the rate enhancement index denoted as $(R_{catalyst} - R_{none})/R_{none}$ was compared with the precipitated iron (Table 3) and the exchanged calcium (Table 8), the latter showed a higher enhancement index; the value for the Ca from aragonite was 3.5 times that for the Fe(cal) catalyst precipitated by using $Ca(OH)_2$. It can thus be concluded that $CaCO_3$ is most promising as a catalyst raw material for steam gasification of low-rank coals. The fluidized bed gasification of YL coal with pressurized steam has shown that ion-exchanged Ca catalyst is suitable for producing H_2-rich gas without tarry materials [47]. On the other hand, the precipitated iron from $FeCl_3$ can catalyze efficiently the pressurized hydrogasification to produce CH_4 from brown coal at a temperature as low as 800 K [23].

4. Conclusions

Steam gasification of coals with inexpensive iron or calcium compounds as catalyst raw materials has been carried out with a thermobalance under atmospheric pressure. The conclusions are summarized as follows:

1. $FeCl_3$, as the major component in acid wastes, is almost inactive when impregnated with brown coal. On the other hand, precipitation methods using several bases can convert $FeCl_3$ to Cl-free, active iron catalysts. The use of $Ca(OH)_2$ provides the most active iron, which leads to ca. twentyfold rate enhancement at 1023 K.
2. The precipitated catalysts exist as fine particles of FeOOH, which are transformed into the highly dispersed Fe_3O_4 upon devolatilization in steam. The crystalline form is retained during char gasification, and Fe_3O_4 particles derived from the most active iron agglomerate at the lowest rate.
3. $Ca(OH)_2$ promotes the gasification at 973 K of all the coals examined when kneaded in water, but the catalytic effect depends strongly on coal type. The calcium can work more effectively for low-rank

coals with higher contents of oxygen-functional groups as ion-exchangeable sites.

4. The Ca ions in $CaCO_3$ readily undergo ion-exchange reactions with COOH groups in low-rank coals in water to form exchanged Ca and CO_2. The extent of the exchange is larger with aragonite naturally present in seashells than with calcite from limestone.
5. The exchanged catalyst shows an exceptionally high activity for the gasification at 973 K of brown coal, poor in inherent minerals, and achieves 40–60-fold rate enhancement, which is larger than that observed for the precipitated iron. Thus, $CaCO_3$ is the most promising catalyst material for steam gasification of low-rank coals.

Acknowledgements

The present work was supported in part by the Tanikawa Fund Promotion of Thermal Technology and by a Grant-in-Aid for Scientific Research from the Ministry of Education, Science, Sports and Culture, Japan. The authors gratefully acknowledge the assistance of Ms. Fumie Hamaoka, Ms. Naoko Yoshida, Ms. Naomi Katahira, Ms. Ayumi Shoji, and Ms. Hazuki Satake in carrying out experiments. We also thank Professors Akira Tomita, Yoshiyuki Nishiyama, and Masashi Iino of our Institute for their helpful discussions and suggestions. Yallourn and Loy Yang coals were kindly supplied from the Coal Corporation of Victoria (now incorporated into HRL Technology Ltd.), Australia.

References

[1] J.L. Figueiredo, J.A. Moulijn (Eds.), Carbon and Coal Gasification, NATO ASI Series, Martinus Nijihoff Publishers, Dordrecht, 1986.
[2] J. Lahaye, P. Ehrburger (Eds.), Fundamental Issues in Control of Carbon Gasification Reactivity, NATO ASI Series, Kluwer Academic Publishers, Dordrecht, 1991.
[3] J.A. Moulijn, F. Kapteijn (Eds.), Special Issue of the International Symposium "Fundamentals of Catalytic Coal and Carbon Gasification". Fuel 65 (1986) 1324–1478.
[4] D.W. McKee, Chem. Phys. Carbon 16 (1981) 1.
[5] B.J. Wood, K.M. Sancier, Catal. Rev. Sci. Eng. 26 (1984) 233.
[6] J.E. Gallagher Jr., C.A. Euker Jr., Energy Res. 4 (1980) 137.
[7] R.L. Hirsch, J.E. Gallagher Jr., R.R. Lessard, R.D. Wesselhoft, Science 251 (1982) 121.
[8] A. Tomita, Y. Ohtsuka, Y. Tamai, Fuel 62 (1983) 150.
[9] Y. Ohtsuka, A. Tomita, Y. Tamai, Appl. Catal. 28 (1986) 105.
[10] A. Tomita, Y. Watanabe, T. Takarada, Y. Ohtsuka, Y. Tamai, Fuel 64 (1985) 795.
[11] T. Takarada, J. Sasaki, Y. Ohtsuka, A. Tomita, Y. Tamai, Ind. Eng. Chem. Res. 26 (1987) 627.
[12] K.J. Hüttinger, J. Adler, G. Hermann, in J.L. Figueiredo, J.A. Moulijn (Eds.), Carbon and Coal Gasification, NATO ASI Series, Martinus Nijihoff Publishers, Dordrecht, 1986, p. 213.
[13] J.L. Johnson, Catal. Rev. Sci. Eng. 14 (1976) 131.
[14] Y. Ohtsuka, Y. Tamai, A. Tomita, Energy Fuels 1 (1987) 32.
[15] Y. Ohtsuka, K. Asami, Ind. Eng. Chem. Res. 30 (1991) 1921.
[16] K. Asami, Y. Ohtsuka, Ind. Eng. Chem. Res. 32 (1993) 1631.
[17] S. Kasaoka, Y. Sakata, H. Yamashita, T. Nishino, J. Fuel Soc. Japan 58 (1979) 373 (Int. Chem. Eng. 21 (1981) 419).
[18] J. Adler, K.J. Hüttinger, Fuel 63 (1984) 1393.
[19] T. Nabatame, Y. Ohtsuka, T. Takarada, A. Tomita, J. Fuel Soc. Japan 65 (1986) 53.
[20] Y. Ohtsuka, A. Tomita, Fuel 65 (1986) 1653.
[21] E.J. Hippo, R.G. Jenkins, P.L. Walker Jr., Fuel 58 (1979) 338.
[22] E. Furimsky, P. Sears, T. Suzuki, Energy Fuels 2 (1988) 634.
[23] Y. Ohtsuka, K. Asami, T. Yamada, T. Homma, Energy Fuels 6 (1992) 678.
[24] K. Asami, P. Sears, E. Furimsky, Y. Ohtsuka, Fuel Process. Technol. 47 (1996) 139.
[25] P.S. Cook, J.D. Cashion, Fuel 66 (1987) 661.
[26] E. Matijevic, P. Scheiner, J. Colloid Interface Sci. 78 (1978) 509.
[27] S. Kaneko, S. Ozeki, K. Inouye, J. Chem. Soc. Jpn., (1985) 1351.
[28] H. Mori, K. Asami, Y. Ohtsuka, Energy Fuels 10 (1996) 1022.
[29] L. von Bogdandy, H.-J. Engell, The Reduction of Iron Ores – Scientific Basis and Technology, Springer-Verlag, New York, NY, 1971, p. 243, English edn.
[30] Y. Ohtsuka, Y. Kuroda, A. Tomita, Y. Tamai, Fuel 65 (1986) 1476.
[31] T. Suzuki, K. Inoue, Y. Watanabe, Energy Fuels 2 (1988) 673.
[32] Y. Ohtsuka, A. Tomita, in D.L. Wise, Y.A. Levendis, M. Metghalchi (Eds.), Calcium Magnesium Acetate: An Emerging Bulk Chemical for Environmental Applications, Elsevier, Amsterdam, 1991, Chap. 10, p. 253.
[33] Y. Ohtsuka, K. Asami, Energy Fuels 9 (1995) 1038.
[34] E.J. Hippo, P.L. Walker Jr., Fuel 54 (1975) 245.
[35] T. Takarada, Y. Tamai, A. Tomita, Fuel 64 (1985) 1438.
[36] K. Otto, L. Bartosiewicz, M. Shelef, Fuel 58 (1979) 565.
[37] H. Freund, Fuel 65 (1986) 63.
[38] L.R. Radovic, A.A. Lizzio, H. Jiang, in J. Lahaye, P. Ehrburger (Eds.), Fundamental Issues in Control of Carbon Gasification Reactivity, NATO ASI Series, Kluwer Academic Publishers, Dordrecht, 1991, p. 235.
[39] A. Linares-Solano, C. Salinas-Martínez de Lecea, D. Cazorla-Amorós, J.P. Joly, in J. Lahaye, P. Ehrburger (Eds.), Fundamental Issues in Control of Carbon Gasification Reactivity, NATO ASI Series, Kluwer Academic Publishers, Dordrecht, 1991, p. 409.

[40] T. Kyotani, S. Hayashi, A. Tomita, Energy Fuels 5 (1991) 683.
[41] T. Rosenqvist, Trans. AIME 191 (1951) 535.
[42] Y. Ohtsuka, K. Asami, in P.R. Dugan, D.R. Quigley, Y.A. Attia (Eds.), Coal Science and Technology, Vol. 18, Elsevier, Amsterdam, 1991, p. 139.
[43] Y. Ohtsuka, K. Asami, Energy Fuels 10 (1996) 431.
[44] G.P. Huffman, F.E. Huggins, R.G. Jenkins, A. Piotroswski, F.W. Lytle, R.B. Greegor, Fuel 65 (1986) 1339.
[45] L.R. Radovic, P.L. Walker Jr., R.G. Jenkins, J. Catal. 82 (1983) 382.
[46] C. Salinas-Martínez de Lecea, M. Almela-Alarcón, A. Linares-Solano, Fuel 69 (1990) 21.
[47] T. Takarada, Y. Ohtsuka, A. Tomita, J. Fuel Soc. Japan 67 (1988) 683.